

MODELING OF PATELLA HEIGHT WITH DISTAL FEMUR AND PROXIMAL TIBIA REFERENCE POINTS WITH ARTIFICIAL NEURAL NETWORK

İLHAN OTAĞ*, KAAAN ÇİMEN*, YUNIS TORUN†,‡,§, ÖZHAN PAZARCI§, SERKAN
AKKOYUN*,¶, AYNUR OTAĞ|| and MEHMET ÇİMEN*

*Department of Anatomy, Faculty of Medicine
Sivas Cumhuriyet University, Sivas, Turkey

†Department of Electric-Electronics Engineering
Sivas Cumhuriyet University, Sivas, Turkey

‡Artificial Intelligence Systems and Data Science
Application and Research Center
Sivas Cumhuriyet University, Sivas, Turkey

§Department of Orthopedics and Traumatology
Sivas Cumhuriyet University, Sivas, Turkey

¶Department of Physics, Faculty of Sciences
Sivas Cumhuriyet University, Sivas, Turkey

||Department of Physiotherapy, Faculty of Health Sciences
Sivas Cumhuriyet University, Sivas, Turkey
**iotag@cumhuriyet.edu.tr

Received 10 April 2021

Accepted 23 January 2022

Published 25 March 2022

The patellofemoral joint is one of the parts of the knee extension mechanism that plays a role in the stability of the knee by enlarging the force arm of the quadriceps muscle and changing the direction of the muscle strength. For the entire knee joint to perform its task painlessly and functionally, the positions and strength of the muscles, the strength of the ligaments, and their reaction to movement must be compatible. The Insall-Salvati (Ins-Sal) index is useful for showing changes in patellar height produced by repositioning the tibial plateau, in other words, showing changes in patellar tendon length. Patella height is an important value to be taken into account in knee prosthesis surgery, tibial osteotomy, and anterior cruciate ligament reconstruction. The morphometric relationship between the reference measurements of the distal femur and proximal tibia and the position of the patella will be useful in determining the natural anatomy. In this study, we aimed to determine the relationship between patella height and distal femur and proximal tibia reference areas by using the artificial neural network method as an alternative approach method. In order to assess the performance of the estimation of the Ins-Sal index, the four ANN model with six input combinations which included age, gender and the reference measurements for the right and left sides have been constructed and tested. The MSE and r values are calculated for every four models for the training and test phase. The results

**Corresponding author.

show that the proposed approach for modeling of relation between reference measurements and the Ins-Sal index is a powerful approach.

Keywords: Morphometry; ligamentum patella; Insall–Salvati; artificial neural network.

1. Introduction

The patella is a sesamoid bone within the quadriceps muscle tendon. The basic task of the patella is to provide a mechanical advantage in the rotation effect by extending the extensor force arm by keeping the force created by the quadriceps muscle away from the rotation center of the knee and changing the direction of this force through the patellar tendon.¹ Length of the patellar tendon and patella morphometry is one of the factors governing the effect of these forces. The total patellar surface is 12–13 cm². Usually, patellofemoral contact starts at 20° of flexion, while earlier or later onset is related to the length of the patellar tendon.^{1,2} In order for the entire knee joint to perform its task painlessly and functionally, the positions and strength of the muscles, the strength of the ligaments, and their reaction to movement must be compatible. Furthermore, morphometric harmony between the patella, femur, and tibia is also important for the healthy entire knee joint. In the bone arrangement, the mediolateral and proximal-distal positions of the patella are one of the research topics in recent literature.^{3–7}

After the introduction of the first measurement method of patellar height by Janssen in 1929, many methods on patellar height have been proposed.⁸ The most known methods used in patellar height measurements have been proposed as Insall–Salvati,⁴ modified Insall–Salvati,⁹ Caton–Deschamps,¹⁰ Blackburn–Pell,¹¹ Carvalho,¹² and Koshino.¹³ Insall–Salvati sought a method that would not be affected by the physical size of the knee, the amount of radiological magnification, and the degree of flexion. They introduced the ratio of the diagonal length of the patella to the patellar tendon length. This ratio has been accepted as almost a universal standard after the research work.¹⁴ The Insall–Salvati (Ins-Sal) index is useful for showing changes in patellar height produced by repositioning the tibial plateau, in other words, showing changes in patellar tendon length.¹⁵

The Ins-Sal index is one of the most commonly used indices in determining the height of the patella. The height of the patella depends on the length of the patellar tendon, the intraoperative shortening of the distance between the patella and the tibial plateau,¹⁶ and the distance between the joint line and the posterior offset of the tibial implant.¹⁷ Patella height measurements generally measure the position of the patella with the tibia.^{4,9–11} In addition, the line reflected from the intercondylar notch, the plateau-patella angle,¹⁴ and the reference point in the distal femur are among the methods used in patellar height measurements.¹⁸

Patella height is an important value to be taken into account in knee prosthesis surgery, tibial osteotomy, and anterior cruciate ligament reconstruction.^{4,19,20} In this study, we aimed to determine the relationship between patella height and distal

femur and proximal tibia reference areas by using the artificial neural network (ANN) method as an alternative approach method. In recent years, ANN method has been accepted as a powerful tool for function approximation and pattern recognition tasks in many real-world problems. ANN has been widely used in the bio-engineering and biomechanics fields,²¹ such as assessing parameters of gait symmetry,²² modeling leg and monofin movements,²³ prediction of lower extremities' movement,²⁴ bone fracture healing assessment,²⁵ classifying hand motions,²⁶ classification of forefoot pain based on plantar pressure measurements,²⁷ classification of gender-specific dynamic gait patterns by using the ANN method,²⁸ Böhler and Gissane angles of the calcaneus²⁹ and determination of patellar position by neural network method.³⁰ As a mathematical model, ANN mimics the brain functionality to solve problems as function approximation, pattern recognition. In this study, two different measurements in the patella region, age, and gender information were used as input of the ANN while network output approximates the Ins-Sal index according to the given inputs. In this study, the Ins-Sal index was obtained for the first time by the ANN method. It was shown that the method is also useful for the problem. In our study, we believe that the morphometric relationship between the reference measurements of the distal femur and proximal tibia and the position of the patella will be useful in determining the natural anatomy.

2. Materials and Method

2.1. Material

This research is a descriptive radio-anatomical study conducted through a retrospective examination of radiographs. Knee measurements of 150 females and 150 males were included in the study. In order to minimize the error in the measurements, samples were selected from individuals whose knee problems were not reported. The distal femur and proximal tibia measurements have been performed by measuring the right and left sides of each gender separately. In order to minimize the error in the measurements, the measurements were repeated twice by the same operator. The average age of the samples measured is 32.96 (in the range of 16–50).

The measurements were made on the anterior–posterior and lateral radiographs of the samples (Fig. 1). The data set consists of the parameters of ligamentum patella length (LP), Ins-Sal index, the line tangential to the lowest point of the femoral condyles (TCL), bicondylar width (BCW), fossa intercondillaris width (NW), tibia width (TW), and intercondylar eminence width (EW). Patella length (PL) is the length measured between the basis and apex of the patella. LP is the determination of the length of the lig. patellae by measuring the distance between the patella apex and the upper part of the tuberositas tibia. Ins-Sal is the calculation of patella height depending on the ratio of LP to PL. BCW is the width parameter of the femoral condyles. NW is the parameter located on the bicondylar width line by which the fossa intercondylar width is calculated. TW is the parameter for the length of the

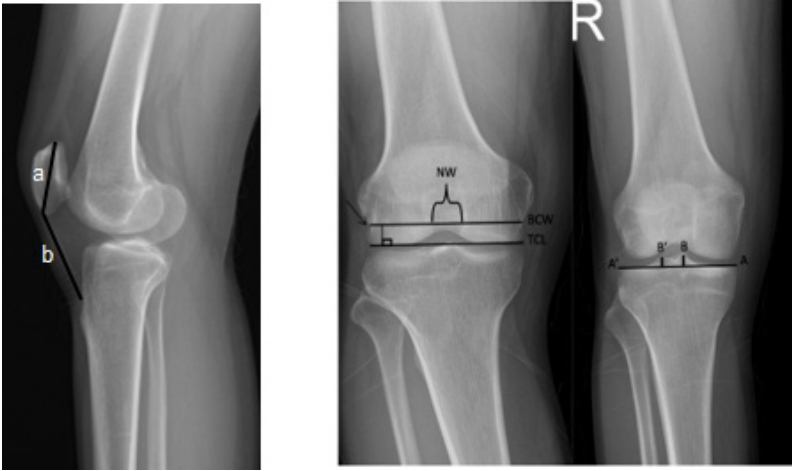


Fig. 1. (Left panel) Ins-Sal index measurement. a: the distance between apex and basis patella which corresponds to patella length (PL), b: the distance between the apex of the patella and tibial tuberosity which corresponds ligamentum patella length (LP), b/a : Ins-Sal index. (Right panel) TCL: the line tangential to the lowest point of the femoral condyles, BCW: the bicondylar width line passing through the sulcus popliteus and parallel to the TCL line, NW: the section where the width of fossa intercondylar on the TCL line is measured. A: the most medial part of the tibia proximal plateau, A': the most lateral part of the tibia proximal plateau, B: eminentia intercondylar tuberculum medial, B': intercondylar eminence tuberculum laterale. Tibia Width (TW): A-A', eminence width (EW): B-B'.

proximal articular surface of the tibia. EW is the parameter of the width between tuberculum intercondylar medial and lateral in intercondylar eminence tibia. The data obtained from our study were uploaded to the SPSS 23.0 program and when the parametric test assumptions were fulfilled (Kolmogorov–Smirnov) in the evaluation of the data, the significance test of the difference between the two means was used when comparing the measurements obtained from two independent groups. To determine differences between two independent groups two-tailed t -test has been conducted. Each stage of the research was conducted under ethical principles. Written permission was obtained from Sivas Cumhuriyet University Non-Invasive Clinical Research Ethics Committee (dated 05.12.2018, numbered 2018-12/12) (Annex. 1) before starting the application. The research was carried out by the Helsinki declaration which is a set of ethical principles regarding human experimentation developed.

2.2. Method

In order to estimate Ins-Sal index, the ANN method was used as an alternative tool. The main task of the ANN is to give outputs in consequence of the computation of the inputs. ANN is a mathematical model mimicking brain functionality and composed of several processing units called neurons. The neurons are located in different

layers as input, hidden, and output. The neurons in each layer are connected to each neuron in the next layer via adaptive synaptic weights.³¹ The input layer neurons receive the data from the environment and the data are transmitted to the output layer neurons through hidden layer neurons. Then corresponding output data are given by the output neurons. The multi-layered Feed-forward neural network architecture is used in this study. The architecture is chosen for the Ins-Sal index modeling due to there was no need to feed past input–output values as inputs to the network.

In order to assess different input combination effects on the correct estimation of Ins-Sal index, four identical models have been trained and tested with six different input combinations to form six-input two-output model. Gender and age have been included for each input combination as the first two inputs. The third and fourth inputs have been selected as LP right and LP left. The remaining two inputs have been selected as one of the BCW, NW, EW for right and left measurements. BCW and NW from the distal femur measurements in the bone arrangement of the knee joint, and for TW and EW from proximal tibia measurements. Therefore, the proposed network architecture consists of one input layer with four neurons ($p = 6$) which correspond to six inputs of each model. The other parts of the network consist of one hidden layer with four ($h = 4$) neurons in each and one output layer with two neurons ($r = 2$), which correspond to the left and right Ins-Sal indexes. The proposed architecture of Multilayer Feed-forward ANN is shown in Fig. 2. There is no rule to take the numbers of the hidden layer and its neurons. After several trials, the number of hidden layers and the number of neurons in the hidden layer were determined in this study. The total number of adjustable weights (w) was 32 according to the

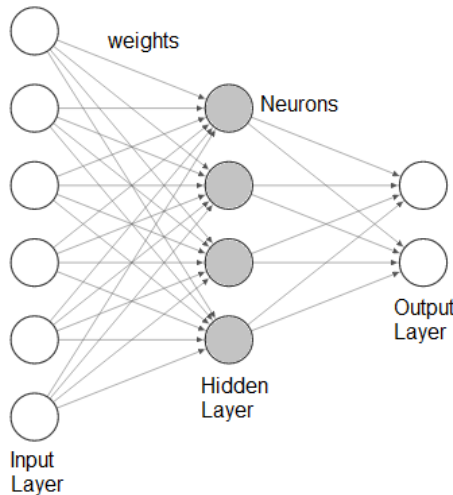


Fig. 2. The used layered Feed-forward ANN structure (6-4-2) for the estimation of Ins-Sal index. The neurons in each layer are connected to the next layer neurons by adaptive synaptic weights.

formula given by

$$w = p \times h + h \times r, \tag{1}$$

where $p = 6$, $h = 4$ and $r = 2$ are the neuron numbers in the input, hidden and output layers, respectively.

A hidden layer is needed for the approximation of any nonlinear function like in this study. The activation function of neurons in the layer can be any well-behaved nonlinear function. In this work, we have chosen tangent hyperbolic activation function³² whose formula is given by

$$\tanh x = \frac{e^x - e^{-x}}{e^x + e^{-x}}. \tag{2}$$

Five fold-cross validation techniques have been performed to divide the training and test data. It produces training and test data sets with 80% of total data as training and 20% of total data as test randomly to form five different combinations of training and test dataset. The number of total data samples for this study is 300; therefore, the network is trained with 236 data points and tested with 64 data points for each of the five loops. For the training stage, the algorithm was a back-propagation algorithm with Levenberg–Marquardt algorithm.^{33,34} By appropriate modifications, ANN modifies its all weights until an acceptable error level between estimated and desired outputs. The difference between the different output values was measured by mean square error (MSE) given by

$$\text{MSE} = \frac{1}{N} \sum_{i=1}^N (d_i - y_i)^2, \tag{3}$$

where N is the number of training data points and d_i and y_i are the desired output and ANN output, respectively. After training the ANN with final weights, the network performance is tested on the test data points which are not given to the network in the training stage. In this work, the performance evaluation has been performed with MSE and correlation coefficient (r) calculation for both the training and test phase. If the estimations of the test data are still sufficiently good enough, ANN is considered to have learned the functional relationship between input and output data of the problem.

3. Results

Right and left side measurements were made for BCW, NW, TW and EW. Comparisons of the right and left sides and the sexes were made in terms of these parameters (Table 1).

This study was repeated with four different input parameter sets and compared to each other to see which set would give better results in obtaining the best Ins-Sal index. In all sets, LP right, LP left, age, and gender data are common parameters. In the first set, BCW right and BCW left data, in the second set, NW right and NW left

Table 1. The measured data for reference points of knee.

Parameter	Side	Gender	Average (mm)	Standard deviation (mm)	Significance value
PL	Right	Female	43.8	3.5	$P = 0.001^*$
		Male	49.8	3.6	
LP	Left	Female	43.9	3.7	$P = 0.001^*$
		Male	50.5	4.4	
	Right	Female	45.9	7.2	$P = 0.015$
		Male	48.1	8.0	
Left	Female	45.4	7.1	$P = 0.005$	
	Male	48.1	9.0		
Ins-Sal	Right	Female	1.0	0.2	$P = 0.001^*$
		Male	0.963	0.2	
	Left	Female	1.0	0.2	$P = 0.001^*$
		Male	0.948	0.2	
BCW	Right	Female	72.8	4.9	$P = 0.001^*$
		Male	84.7	5.2	
	Left	Female	72.4	5.1	$P = 0.001$
		Male	84.2	5.0	
NW	Right	Female	16.8	2.6	$P = 0.001^*$
		Male	20.8	2.5	
	Left	Female	17.8	2.8	$P = 0.001^*$
		Male	21.1	2.9	
TW	Right	Female	75.9	4.8	$P = 0.001^*$
		Male	86.7	4.9	
	Left	Female	75.9	4.8	$P = 0.001^*$
		Male	86.8	5.2	
EW	Right	Female	11.1	2.1	$P = 0.014$
		Male	11.8	2.4	
	Left	Female	10.9	2.3	$P = 0.098$
		Male	11.4	2.2	

Note: *Statistically the difference is significant.

data, in the third set, EW right and EW left data, and in the fourth set, TW right and TW left data were included among the input parameters.

In Table 2, the inputs of these four different sets and the mean values of MSE and correlation coefficient (r) on the training and test data are listed according to the side

Table 2. Four different ANN input parameters and their results on the data.

ANN inputs	Side	MSE		r	
		Training	Test	Training	Test
BCW + LP + Age + Gender	Right	0.004	0.005	0.938	0.890
BCW + LP + Age + Gender	Left	0.005	0.008	0.941	0.898
NW + LP + Age + Gender	Right	0.005	0.007	0.926	0.869
NW + LP + Age + Gender	Left	0.005	0.006	0.934	0.890
EW + LP + Age + Gender	Right	0.006	0.007	0.929	0.886
EW + LP + Age + Gender	Left	0.005	0.008	0.938	0.888
TW + LP + Age + Gender	Right	0.004	0.008	0.946	0.898
TW + LP + Age + Gender	Left	0.004	0.005	0.954	0.915

of the bone. It is seen that the results obtained by using different input parameters give different MSE and r values. In addition, MSE and r values were obtained differently in the estimates of right and left side measurements. In the estimates on the training data in the sets that included BCW or NW as the ANN's inputs, the MSE values of the right side were lower than the left side, but in the case of EW or TW among the inputs, the predictions for the left side were more successful. In similar examinations on test data, the MSE value was smaller for the right side in the calculations where BCW or EW was taken as the input parameter, while the left side had a smaller MSE value in the calculations where NW or TW was input.

Figure 3 shows the comparison of the predictions on the training data with the measured values. As can be seen from the figure, the difference between the measured value and ANN estimates is concentrated around the zero line but spreads between approximately -0.2 and $+0.2$ values. In the upper left panel of the figure, you can see the results of the ANN structure in which BCW is included in the inputs. In the estimation of the Ins-Sal index, this ANN showed a maximum deviation of 0.252 mm for the left side and -0.265 mm for the right side. In the upper right panel, the results are shown when the NW parameter is included in the ANN inputs. Looking at the results obtained in this case, it is seen that the maximum deviations of the ANN values from the measured values are 0.309 mm for the left side and -0.265 mm for the right side. The results of the ANN structure, in which EW is included as the input parameter, are presented in the lower-left panel. It is seen that the maximum

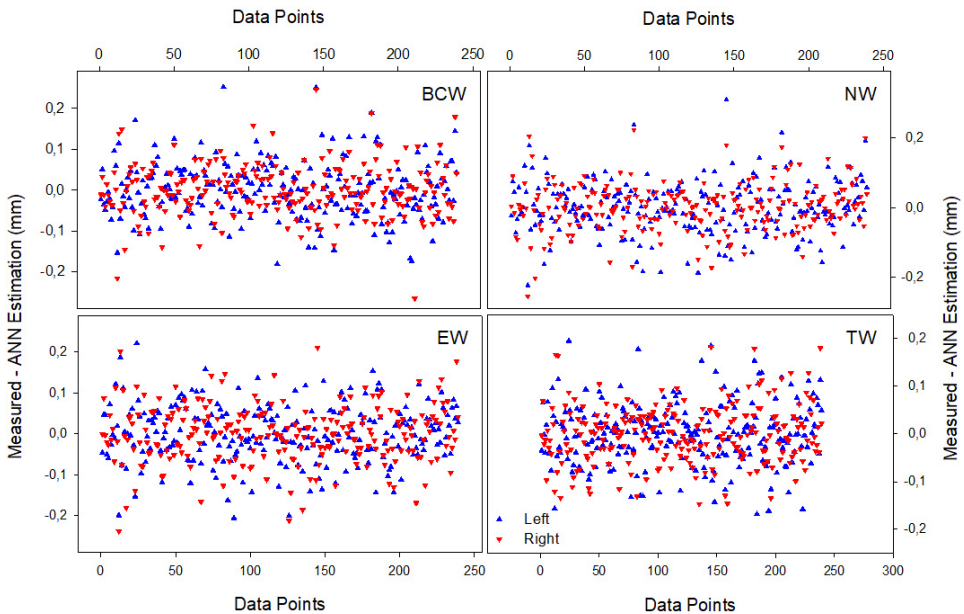


Fig. 3. The deviations between the actual measured Ins-Sal indexes and the estimated Ins-Sal indexes with ANN for training data points.

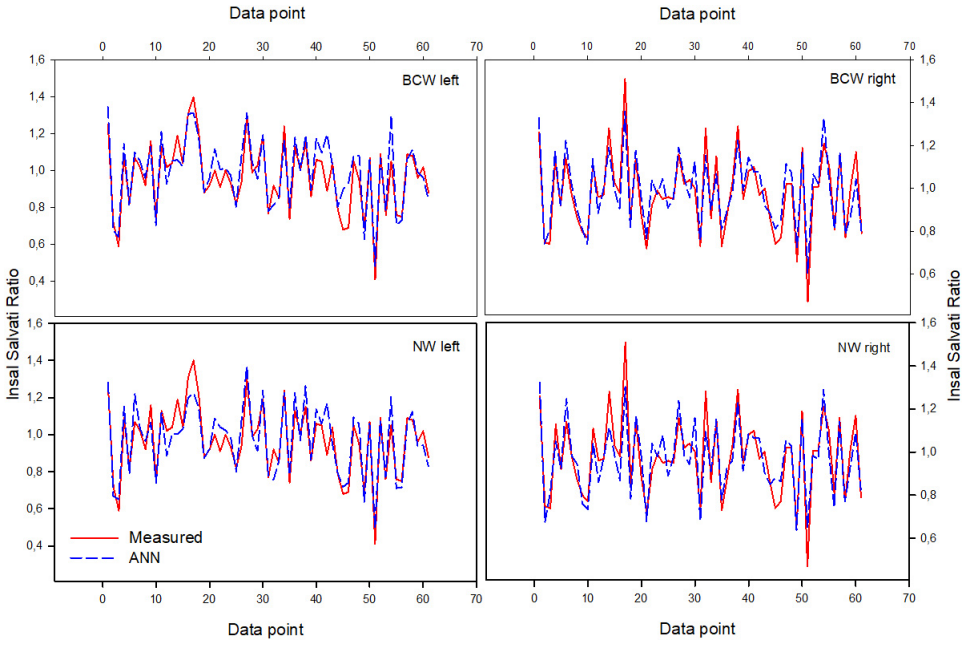


Fig. 4. Measured and ANN estimated Ins-Sal index on the test data points.

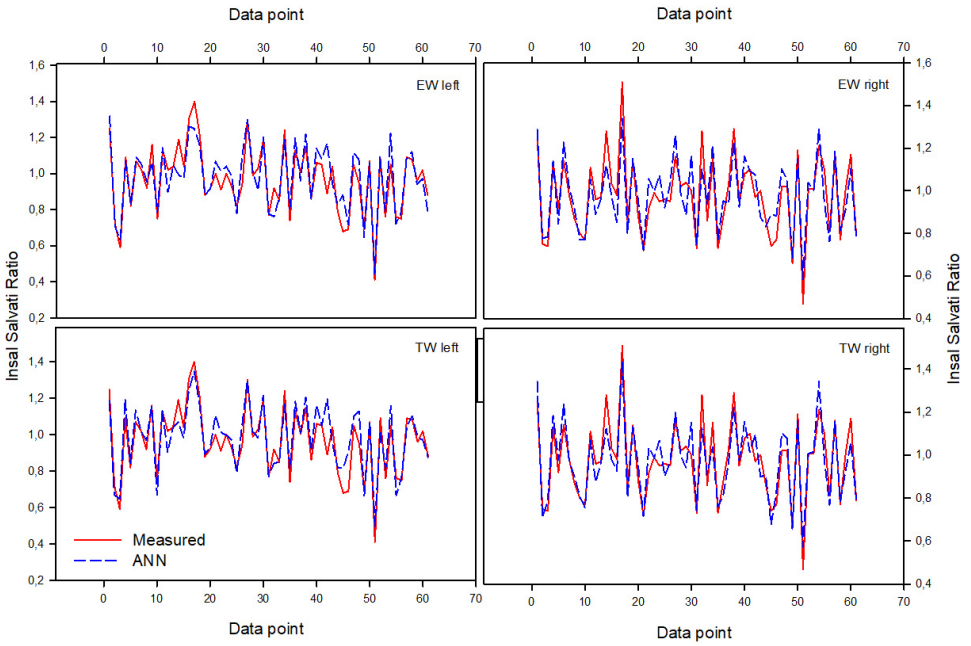


Fig. 5. Same as Fig. 4 but for different ANN inputs.

deviations from the measured values are 0.222 mm for the left side and -0.238 mm for the right side. Finally, in the bottom right panel, the results of the calculations that include TW in the ANN inputs are given. When the maximum deviations in this situation are examined, it is seen that the result is obtained with deviations of 0.195 mm for the left side and 0.182 mm for the right side.

In Figs. 4 and 5, the results of ANN predictions in the test data set are presented. Considering the plots drawn separately for the right and left sides, the agreement between the measured value of the Ins-Sal index and the ANN predicted value is seen in the plots drawn together. Considering the fact that the data are very nonlinear, the ANN estimator gives such successful results, indicating that this method is suitable in determining the Ins-Sal index.

4. Discussion

The main objective of the study is to achieve an artificial intelligence model which could estimate the patella position according to reference measurements of the distal femur and proximal tibia of a healthy person. The patella collects the forces from the four heads of the quadriceps into the middle and transmits them to the tibia in the most frictionless way through the patellar tendon.¹ The position of the patella in the patellofemoral joint and its harmony with the femur is important for the joint mechanism.

While the patella comes from full flexion to full extension, it travels 7 cm in the proximal-distal direction.³⁵ Patellar height is an important factor in patellar tracking and changes the strength of the patellofemoral joint reaction. Patella alta is a condition associated with patellofemoral malalignment and a reduced patellofemoral contact area, leading to patellofemoral pain or instability.^{36,37} Patella baja limited knee opening is associated with Osgood–Schlatter disease and patellar arthritis.³⁸ The position of the patella in a position other than its normal position causes many discomfort situations. Therefore, studies among the muscle, ligament and bone structures related to the position of the patella continue to be the subject of many studies.

In our study, the relationship between patellar height and BCW and NW in distal femur reference measurements and TW and EW, which are the reference measurements of the proximal tibia, were investigated. It is clear that there is a significant correlation between the proximal tibia, distal femur, and patella bone morphometries. This correlation must continue for the whole knee joint to perform properly. It is possible to encounter various problems when the harmony in the whole knee joint is broken. Surgery may be required to provide mechanical treatment of the knee joint when this harmony is broken in situations of discomfort. In the planning of this operation, the relationship between the proximal tibia, distal femur, and patella morphometry would be among the guiding factors.

The kinematics of the knee joint are very different from simple flexion and extension movements. Femur expresses the relationship between the patella and the

tibia during kinematic knee movement. Joint surface, meniscus, and ligament structures determine the normal kinematic relationship between femur patella and tibia. The intended target is to get a painless knee capable of maximum movement and with proper alignment.³⁹

In our results from ANN method, as can be seen from Table 2, in the estimation of the Ins-Sal index on the right in the training data points, the ANN structure including the BCW parameter in the input set gave the best results with 0.004 MSE value. For the left, the best result as 0.0037 MSE value has been obtained by the ANN structure including the TW parameter in the input set. The corresponding r values are 0.94 and 0.95, respectively. In the predictions made on the test data points, the ANN structure in which BCW was included in the inputs gave the best results for the right side with a 0.005 MSE value, while the ANN structure with NW included in the inputs gave the best results with 0.0064 MSE value for the left side. The corresponding r values were obtained as 0.94 and 0.90, respectively.

In the predictions made on the training data, the results with the highest MSE value were obtained in sets with EW among the input parameters. These MSE values are 0.006 and 0.005 for the right and left sides, respectively. The corresponding r values are 0.93 and 0.94, respectively. The results with the largest MSE on the test data were obtained with the set in which TW is included in the input parameter for the right side, and with the set including EW for the left side. These MSE values are also 0.008 and 0.008, respectively. The corresponding r value was calculated as 0.89 for both. Although they have higher MSE values compared to each other, the results of the studies performed with all four parameter sets are thought to be successful in predicting the Ins-Sal index.

In our study, the relationship was tried to be explained by using the fundamental measurements between the distal femur, proximal tibia, and patella morphometry. The results were obtained when significant reference lengths were used at the knee joint instead of the patella length used to measure the patella height. These results illustrate that there is a morphometric fit between the bone reference lengths that are functionally related to the knee joint. We believe that determining this harmony numerically is important for knee mechanics and restructuring studies.

The natural arrangement of the individual is aimed at total knee arthroplasty. Patients whose natural arrangement is structurally abnormal on the neutral mechanical axis cannot be functionally comfortable after total knee arthroplasty.⁴⁰ In our study, we believe that the morphometric relationship between the reference measurements of the distal femur and proximal tibia and the position of the patella will be useful in determining the natural anatomy.

One of the most common problems after total knee arthroplasty is patellar instability and patellofemoral incompatibility. For a successful patella fit, providing the normal Q angle, placement of all components in proper rotation, and ensuring normal patellofemoral tension are important factors. One of the factors affecting the patellar placement is the size and location of the femur and tibia components.⁴⁰ In total knee arthroplasty, the proper patellofemoral arrangement is possible with the

mechanical and positional balance between components.⁴⁰ Patellar position and bone morphometry show significant changes according to gender and the difference between the right and left sides. In our study, the patellar height and the distal femur, proximal tibia measurements were studied considering the gender and side difference. There is a higher patella in women than that of men. In our study, we have obtained for women that the patella heights are 1.04 and 1.03 for the left and right sides, respectively. For men, the patella heights were obtained 0.96 and 0.95 for the left and right sides, respectively. Thus, it can be used to get better results in the relationship between all knee mechanics and restructuring studies by considering the gender and side difference.

5. Conclusion

If we consider the knee joint as a mechanism consisting of bone, cartilage, capsule, and ligaments, the relationship between the bones will contribute to our understanding of knee biomechanics. It will be useful in patellar height planning compatible with the distal femur and proximal tibia measurements to determine the natural anatomical alignment of the individuals. In our study, an alternative method with ANN for modeling the morphometric relationship between the reference measurements of the distal femur and proximal tibia and the position of the patella will be useful in determining the natural anatomy.

The research focuses on the vertical position of the patella. However, there are some factors on patella height as the position of *mediolateral* patella, partial patella, and status of the ligaments of the patella. We believe that the proposed approach would be useful for the research work related to the patella position. The proposed approach on estimating patella height with ANN also could help the research topics as that restructuring of patellar fractures,⁴¹ restructuring of anterior cruciate ligament,⁴² and diagnosis of some diseases according to patella position.⁴³

References

1. Aglietti P, Giron F, Cuomo P, Disorders of patellofemoral joint, in Scott WN (ed.), *Surgery of the Knee*, 2nd edn., Jaypee Brothers Medical Publishers (P), Ltd., Churchill Livingstone, New York, pp. 2611–2611, 2016.
2. Göncü K, Alt Ekstremité Kinezyolojik Özellikleri, in Beyazova M, Gökçe-Kutsal Y (eds.), *Fiziksel Tıp ve Rehabilitasyon*, Güneş Kitapevi, Ankara, pp. 198–204, 2011.
3. Otağ A, Otağ İ, Sabancıoğulları V, Çimen M, Geometric analysis of medio-lateral position of patella: A new measuring tool, *Niger J Clin Pract* **17**:549–554, 2014, <https://doi.org/10.4103/1119-3077.141415>.
4. Insall J, Salvati E, Patella position in the normal knee joint, *Radiology* **101**:101–104, 1971, <https://doi.org/10.1148/101.1.101>.
5. Conry KT, Cosgarea AJ, Tanaka MJ, Elias JJ, Influence of tibial tuberosity position and trochlear depth on patellar tracking in patellar instability: Variations with Patella Alta, *Clin Biomech* **87**:105406, 2021, <https://doi.org/10.1016/j.clinbiomech.2021.105406>.

6. Salem KH, Sheth MR, Variables affecting patellar height in patients undergoing primary total knee replacement, *Int Orthop* **45**:1477–1482, 2021, <https://doi.org/10.1007/s00264-020-04890-6>.
7. Grandhi TSP, Titus V, The results of patellar stainless steel wire extensor mechanism reconstruction in proximal tibial tumour excision mega-prosthesis surgeries for proximal tibial sarcomas, *Knee* **29**:332–344, 2021, <https://doi.org/10.1016/j.knee.2021.02.014>.
8. Prudhon JL, Caton JH, Aslanian T, Verdier R, How is patella height modified after total knee arthroplasty? *Int Orthop* **42**:311–316, 2018, <https://doi.org/10.1007/s00264-017-3539-6>.
9. Grelsamer RP, Meadows S, The modified Insall–Salvati ratio for assessment of patellar height, *Clin Orthop Relat Res* **282**:170–176, 1992, <https://doi.org/10.1097/00003086-199209000-00022>.
10. Caton J, Deschamps G, Chambat P, Lerat JL, Dejour H, Patella infera. Apropos of 128 cases, *Rev Chir Orthop Reparatrice Appar Mot* **68**:317–325, 1982, <http://www.ncbi.nlm.nih.gov/pubmed/6216535>.
11. Blackburn JS, Peel TE, A new method of measuring patellar height, *J Bone Joint Surg Ser B* **59**:241–245, 1977, <https://doi.org/10.1302/0301-620x.59b2.873986>.
12. de Carvalho A, Andersen AH, Topp S, Jurik AG, A method for assessing the height of the patella, *Int Orthop* **9**:195–197, 1985, <https://doi.org/10.1007/BF00268170>.
13. Koshino T, Ejima M, Okamoto R, Morii T, Gradual low riding of the patella during postoperative course after total knee arthroplasty in osteoarthritis and rheumatoid arthritis, *J Arthroplasty* **5**:323–327, 1990, [https://doi.org/10.1016/S0883-5403\(08\)80091-5](https://doi.org/10.1016/S0883-5403(08)80091-5).
14. Portner O, Pakzad H, The evaluation of patellar height: A simple method, *J Bone Joint Surg Ser A* **93**:73–80, 2011, <https://doi.org/10.2106/JBJS.I.01689>.
15. Portner O, High tibial valgus osteotomy: Closing, opening or combined? Patellar height as a determining factor, *Clin Orthop Relat Res* **472**:3432–3440, 2014, <https://doi.org/10.1007/s11999-014-3821-5>.
16. Grelsamer RP, Patella baja after total knee arthroplasty: Is it really patella baja? *J Arthroplasty* **17**:66–69, 2002, <https://doi.org/10.1054/arth.2002.28728>.
17. Figgie HE, Goldberg VM, Heiple KG, Moller HS, Gordon NH, The influence of tibial-patellofemoral location on function of the knee in patients with the posterior stabilized condylar knee prosthesis, *J Bone Joint Surg Ser A* **68**:1035–1040, 1986, <https://doi.org/10.2106/00004623-198668070-00009>.
18. Chareancholvanich K, Narkbunnam R, Novel method of measuring patellar height ratio using a distal femoral reference point, *Int Orthop* **36**:749–753, 2012, <https://doi.org/10.1007/s00264-011-1340-5>.
19. Simmons E, Cameron JC, Patella alta and recurrent dislocation of the patella, *Clin Orthop Relat Res* **274**:265–269, 1992, <https://doi.org/10.1097/00003086-199201000-00026>.
20. Kesmezacar H, Erginer R, Ogut T, Seyahi A, Babacan M, Tenekecioglu Y, Evaluation of patellar height and measurement methods after valgus high tibial osteotomy, *Knee Surg. Sports Traumatol Arthrosc* **13**:539–544, 2005, <https://doi.org/10.1007/s00167-004-0572-y>.
21. Schöllhorn WI, Applications of artificial neural nets in clinical biomechanics, *Clin Biomech* **19**:876–898, 2004, <https://doi.org/10.1016/j.clinbiomech.2004.04.005>.
22. Michalski R, Wit A, Gajewski J, Use of artificial neural networks for assessing parameters of gait symmetry, *Acta Bioeng Biomech* **13**:65–70, 2011.
23. Rejman M, The elements of modeling leg and monofin movements using a neural network, *Acta Bioeng Biomech* **8**:55–63, 2006.
24. Kutilek P, Farkasova B, Prediction of lower extremities' movement by angle-angle diagrams and neural networks, *Acta Bioeng Biomech* **13**:57–65, 2011.

25. Kaufman JJ, Chiabrera A, Hatem M, Hakim NZ, Figueiredo M, Nasser P, Lattuga S, Pilla AA, Siffert RS, A neural network approach for bone fracture healing assessment, *IEEE Eng Med Biol Mag* **9**:23–30, 1990, <https://doi.org/10.1109/51.59209>.
26. Baspınar U, Varol HS, Senyurek VY, Performance comparison of artificial neural network and gaussian mixture model in classifying hand motions by using sEMG signals, *Biocybern Biomed Eng* **33**:33–45, 2013, [https://doi.org/10.1016/S0208-5216\(13\)70054-8](https://doi.org/10.1016/S0208-5216(13)70054-8).
27. Keijsers NLW, Stolwijk NM, Louwerens JWK, Duysens J, Classification of forefoot pain based on plantar pressure measurements, *Clin Biomech* **28**:350–356, 2013, <https://doi.org/10.1016/j.clinbiomech.2013.01.012>.
28. Andrade A, Costa M, Paolucci L, Braga A, Pires F, Ugrinowitsch H, Menzel HJ, A new training algorithm using artificial neural networks to classify gender-specific dynamic gait patterns, *Comput Methods Biomech Biomed Eng* **18**:382–390, 2015, <https://doi.org/10.1080/10255842.2013.803081>.
29. Khoshhal KI, Ibrahim AF, Al-Nakshabandi NA, Zamzam MM, Al-Boukai AA, Zamzami MM, Böhler's and Gissane's angles of the calcaneus in the Saudi population, *Saudi Med J* **25**:1967–1970, 2004.
30. Otağ I, Otağ A, Akkoyun S, Çimen M, A way in determination of patellar position: Ligamentum patellae angle and a neural network application, *Biocybern Biomed Eng* **34**:184–188, 2014, <https://doi.org/10.1016/j.bbe.2014.02.004>.
31. Kubat M, Neural networks: A comprehensive foundation by Simon Haykin, Macmillan, 1994, ISBN 0-02-352781-7, *Knowl Eng Rev* **13**:409–412, 1999, <https://doi.org/10.1017/s0269888998214044>.
32. Feng J, Lu S, Performance analysis of various activation functions in artificial neural networks, *J Phys Conf Ser* **1237**:022030, 2019, <https://doi.org/10.1088/1742-6596/1237/2/022030>.
33. Levenberg K, A method for the solution of certain nonlinear problems in least squares, *Q Appl Math* **2**:164–168, 1944, <https://doi.org/10.1090/qam/10666>.
34. Marquardt DW, An algorithm for least-squares estimation of nonlinear parameters, *J Soc Ind Appl Math* **11**:431–441, 1963, <https://doi.org/10.1137/0111030>.
35. Mow VC, Flatyow EL, Ateshian GA, Biomechanics, in: Buckwalter JA, Einhorn TA, Simon SR (eds.), *Orthopaedic Basic Science*, 2nd edn., American Academy of Orthopaedic Surgeons, Rosemont, pp. 133–180, 2000.
36. Caton JH, Dejour D, Tibial tubercle osteotomy in patello-femoral instability and in patellar height abnormality, *Int Orthop* **34**:305–309, 2010, <https://doi.org/10.1007/s00264-009-0929-4>.
37. Post WR, Anterior knee pain: Diagnosis and treatment, *J Am Acad Orthop Surg* **13**:534–543, 2005, <https://doi.org/10.5435/00124635-200512000-00006>.
38. Aparicio G, Abril JC, Calvo E, Alvarez L, Radiologic study of patellar height in Osgood-Schlatter disease, *J Pediatr Orthop* **17**:63–66, 1997, <https://doi.org/10.1097/01241398-199701000-00015>.
39. Kayaokay K, Aydoğdu S, Total diz artroplastisinde dizilim, komponent boyut ve yerleşim sorunları, *TOTBID Derg* **18**:220–236, 2019, <https://doi.org/10.14292/totbid.dergisi.2019.26>.
40. Salzmann M, Fennema P, Becker R, Hommel H, Does postoperative mechanical axis alignment have an effect on clinical outcome of primary total knee arthroplasty? A retrospective cohort study, *Open Orthop J* **11**:1330–1336, 2017, <https://doi.org/10.2174/1874325001711011330>.
41. Kim Y, Kwon M, Ryu JY, Moon SW, Biomechanical analysis of the kirschner-wire depth of the modified tension band wiring technique in transverse patellar fractures: An

- experimental study using the finite-element method, *CiOS Clin Orthop Surg* **13**:315–319, 2021, <https://doi.org/10.4055/cios20253>.
42. Goto K, Taketomi S, Shimizu N, Central patellar portal placement frequently provokes anterior knee compartment radiological abnormalities in anterior cruciate ligament reconstruction, *Knee Surg. Sports Traumatol Arthrosc* **28**:2255–2260, 2020, <https://doi.org/10.1007/s00167-019-05817-4>.
 43. Özel D, The relationship between early-onset chondromalacia and the position of the patella, *Acta Radiol* **61**:370–375, 2020, <https://doi.org/10.1177/0284185119861901>.

Copyright of Journal of Mechanics in Medicine & Biology is the property of World Scientific Publishing Company and its content may not be copied or emailed to multiple sites or posted to a listserv without the copyright holder's express written permission. However, users may print, download, or email articles for individual use.